

Evaluation of heating uniformity in radio frequency heating systems using carrot and radish**

Ling Kong¹, Min Zhang^{1,2*}, Yuchuan Wang¹, Benu Adhikari³, and Zaixing Yang⁴

¹State Key Laboratory of Food Science and Technology, Jiangnan University, 214122 Wuxi, Jiangsu, China

²Jiangsu Province Key Laboratory of Advanced Food Manufacturing Equipment and Technology, Jiangnan University, China

³School of Applied Sciences, RMIT University, Melbourne, VIC3083, Australia

⁴Xuzhou Branch, Haitong Food Group Company, Jiangsu Peixian, 221600, China

Received February 15, 2016; accepted September 6, 2016

A b s t r a c t. Lack of heating uniformity is a major problem impeding the broader adaptation of radio frequency heaters in industrial applications. The overall aim of this study was to evaluate the uniformity of heating or temperature distribution within food samples (three different carrot and one radish rectangles) placed vertically and horizontally within a radio frequency heating cavity. The intensity of the electric field in radio frequency was found to be symmetrical. The temperatures at the vertically top positions were lower than the vertically bottom positions at the equidistance from the vertical center with the highest was at the vertically central position. The rate of temperature rise at all the positions were higher in taller (higher mass) than the shorter (lower mass) rectangles of carrots. The temperatures at the corners and edges were lower than at the cross sectionally central positions at all the heights tested in both carrots and radishes. The rate of temperature rise at all the vertical positions was higher in radish rectangles than in the carrot rectangles of the same dimensions. The similarity of temperature distribution in carrot and radish rectangles suggested that the heating patterns and uniformity in carrots and radishes in RF heating were almost the same.

K e y w o r d s: radio frequency, heating uniformity, carrots, radish

INTRODUCTION

Radio frequency (RF) is the rate of oscillation of an electromagnetic wave in the range of 1 to 300 MHz. Radio frequency generates rapid and volumetric heating. Three radio frequencies (*ie* 13.56, 27.12 and 40.68 MHz) are permitted in industrial, scientific and medical applications (Marra *et al.*, 2009). An alternating electric field is deve-

loped between the electrodes of a RF heating oven and the product is placed in between these electrodes. The material placed in an RF heating system is rapidly heated due to friction generated by the alternative movement of molecules and the displacement of the charge within the sample. The heating characteristics and dielectric behaviour of food materials vary with radio frequency and temperature and these variations are significantly affected by moisture and salt contents (Orsat *et al.*, 2004).

Radio frequency is used in food industries in applications such as pasteurization/sterilization (Liu *et al.*, 2014; Luechapattaporn *et al.*, 2005), defrosting (Llave *et al.*, 2015), thawing (Uyar *et al.*, 2015) and drying (Wang *et al.*, 2014a). RF is increasingly being applied in food industries for the better quality attributes of final product compared to conventional thermal treatment (Gao *et al.*, 2010; Tiwari *et al.*, 2008). Ha *et al.* (2013) investigated the efficacy of RF heating in inactivating *S. Typhimurium* and *Escherichia coli* O157:H7 in two types of peanut butter samples (Ha *et al.*, 2013). These authors measured the changes in colour and sensorial perception (texture, flavour and overall acceptability) in peanut butter and cracker samples to determine the effect of RF on quality. When the requirement for the microbial quality was met, the colour and above mentioned sensorial characteristics of peanut butter and cracker samples were not significantly affected by RF treatment. These observations suggested that RF heating can be applied to control pathogens in peanut butter and peanut butter containing products without affecting quality (Ha *et al.*, 2013). RF is also a very promising technology for pasteurization of food materials. For example, Ukuku and Geveke investigated the combined effect of RF and UV-light on the

*Corresponding author e-mail: minlichunli@163.com

**This work was financial supported by China 863 HI-TECH Research and Development Program (No. 2011AA100802), Jiangsu Province (China) 'Collaborative Innovation Center for Food Safety and Quality Control' Industry Development Program, Jiangsu Province (China) Infrastructure Project (Contract No. BM2014051, 2011 to 2017).

cellular injury and inactivation of *Escherichia coli* K-12 in apple juice (Ukuku and Geveke, 2010). The results of this study showed that the combination of RF with UV caused more injury to bacterial cells leading to more leakage of intracellular substances than cells treated with UV-light alone. The application of RF was also found to improve the storability of repacked hams (Orsat *et al.*, 2004). The RF treatment is now considered to be a promising postharvest technology for disinfestation of legumes (Jiao *et al.*, 2012; Wang *et al.*, 2006).

Two major challenges impeding broader application of RF heating in food industry are the non-uniform and runaway heating. They cause localized overheating especially in foods with intermediate and high water content. Hence, the uniformity of heating needs to be improved before RF treatments can find broader commercial application (Alfaifi *et al.*, 2014). There are a number of publications describing which factors affect the heating uniformity and by how much (Romano and Marra, 2008). Mathematical simulations have been used to design RF heating systems used in food processing (Brodie, 1969; Jumah, 2005; Marra *et al.*, 2007; Tiwari *et al.*, 2011b; Wang *et al.*, 2005b). Birla *et al.* (2008a) investigated the effect of dielectric properties, dimension and shape of a sample and the properties of surrounding medium on the temperature distribution within a spherical object placed between two parallel plate RF electrodes using finite element-based numerical simulation program. These authors reported that the simulation results closely followed the experimental data indicating that the numerical simulations can be confidently used to predict the heating pattern of food materials using measurable properties of the sample and surrounding medium. Birla *et al.* (2008b) further developed the numerical simulation program and applied it to characterize the RF heating of fruits having different dielectric properties in peel and core (such as orange, apple, grapefruit, peach and avocado). This study showed that the surface heating was dominant when peel was present and the core heating was dominant when peel was removed and showed that numerical simulation can provide better understanding of RF heating characteristics of fruits. This type of numerical simulations can be useful in assessing the feasibility of RF energy to a given food system.

In the above context, the aim was to evaluate the uniformity of heating or temperature distribution within food samples placed vertically and horizontally within a RF heating cavity, and then three different rectangles of carrot with the same cross sectional area but different heights and one rectangle of radish were used. Among the test three aspects were considered:

- evaluate the heating uniformity at different horizontal positions within the RF cavity,
- evaluate the heating uniformity in vertical direction within the cavity using three carrot rectangles of the same cross section area but different heights,

- compare the heating patterns and heating uniformity in carrot and radish samples within the RF cavity.

MATERIALS AND METHODS

Fresh carrot and radish samples were purchased from a local market located at Xuelang town (Wuxi, China). The dielectric constants ϵ' of these samples were measured at 27.12 MHz and 10°C and were found to be 114.2±4.11 for carrot and 81.4±1.17 for radish samples. The loss factors ϵ'' for carrot and radish samples were 545.3±12.76 and 226.2±6.88, respectively. The penetration depth (d_p) was calculated according to Gao *et al.* (2012) method using equation given below and found to be 5.9 and 9.9 cm for carrot and radish samples, respectively:

$$d_p = \frac{c}{2\pi f \sqrt{2\epsilon' \left[\sqrt{1 + \left(\frac{\epsilon''}{\epsilon'}\right)^2} - 1 \right]}}$$

where: c is the speed of light in free space (3×10^8 m s⁻¹) and f is the frequency (Hz) which is 27.12MHz in the case of RF.

An open-ended coaxial-line probe connected to a network analyzer (E5062A, Agilent Technologies, Malaysia) was used to measure the dielectric constants (ϵ') and loss factors (ϵ'') of the carrot and radish samples at 27 MHz. The network analyzer was calibrated with air, a short-circuit block and deionized water at room temperature. An open ended dielectric probe was used to closely contact the sample. Proprietary software supplied by the Agilent Technologies was used to record and calculate the dielectric properties from acquired data. Experiments were carried out in triplicate and mean values were reported above.

A pilot-scale (6kW, 27.12MHz) radio frequency heating equipment (Model SO6B, Monga Strayfield, United Kingdom) was used to investigate the heating uniformity in carrots. The size of the top (parallel) electrode plate was 83×40 cm. The bottom plate electrode was much larger with a size of 98×59 cm. The gap between the two electrodes was adjusted according to RF power and the dimension of the sample. The vertical gap between the two RF electrodes could be adjusted between 120 to 240 mm. A gap of 120 mm was set throughout this study because smaller gap would generate greater field strength and the temperature would increase faster. An earlier simulation study on the RF heating of wheat flour also suggested that a smaller gap between the electrodes improved the uniformity of RF power (Tiwari *et al.*, 2011a).

Two sets of uniformity tests were carried out to evaluate the effect of horizontal positioning of sample with respect to the two parallel electrodes. In the first set of tests, fresh carrots were cut into small cubes (0.8 × 0.8 × 0.8 cm) and uniformly packed in a plastic tray (59 × 40 cm) which was

subsequently placed on the center of bottom electrode and heated for 5 min using the RF module. At the end of 5 min, the RF power was turned off and the plastic tray was immediately taken out and the temperature of the samples was mapped out by using an infrared thermal imaging camera (IRI 4010 Multi-Purpose Imager, IRISYS, Northampton, UK). The temperature imaging process was completed within 10 s in order to minimize the heat loss to the ambient air.

In the second set of tests, fresh carrots were cut into bigger cubes ($3 \times 3 \times 3$ cm) and then placed them on the bottom plate at the six positions shown in Fig. 1. This positioning of the samples was used to take in to account the fact that the size of the top plate is smaller than that of the bottom one (Fig. 1). Every cube was placed on top of an inverted petri dish (diameter 90 mm, height 15 mm). In this way the distance between the bottom surface of the cubes and the surface of the bottom electrode was 15 mm. This precaution was taken to avoid overheating and burning of sample which usually occurs when a sample contacts the surface of the electrode. A fiber optic temperature probe (FOTS-DINA-2080-NS/N 1448C001, INDIGO PRECISION, Canada) was inserted at the center of each cube to measure the temperature change during heating. The probe measured and recorded the temperature every 6.5 s.

In order to study the heating uniformity of RF in carrots when placed vertically three sets of tests were carried out at position 4 shown in Fig. 1 since materials would be placed from central to edge in factory production lines in most cases.

In the first set of tests, carrots were cut into rectangles ($3 \times 3 \times 6$ cm) and then one piece was placed into the RF cavity in each experiment supported by a petri dish with the height of 15 mm. The fiber optic temperature sensors were inserted within the rectangles at the height of: 1, 2, 3, 4, and 5 cm. The sample was heated using the RF heater for 5 min.

In the second set of tests, slightly longer carrot rectangles ($3 \times 3 \times 8$ cm) were prepared and fiber optic probes were inserted at the heights of 1, 2, 3, 4, 5, 6, and 7 cm. These samples were heated using RF heater for 5 min as described above in the case of $3 \times 3 \times 6$ cm rectangular samples.

In the third set of tests, carrots were cut into even longer rectangles of $3 \times 3 \times 10$ cm and the temperature probes were inserted every 1 cm from 1 to 9 cm. These particular samples were heated for only 2 min using RF because the temperature was found to rise faster in these samples.

Firstly, radish was cut into $3 \times 3 \times 8$ cm rectangles and the other operations for these tests were similar to those carried out in the case of carrots in vertical uniformity tests.

Secondly, carrot and radish samples were cut into $3 \times 3 \times 8$ cm and then divided into four $3 \times 3 \times 2$ cm rectangles. The RF heating was stopped after 150 s to maintain a relatively low sample temperature (eg 50-60°C), which can be used to evaluate the effect of the RF field on the heating patterns as it reduces the heat loss from the sample to the ambient air.

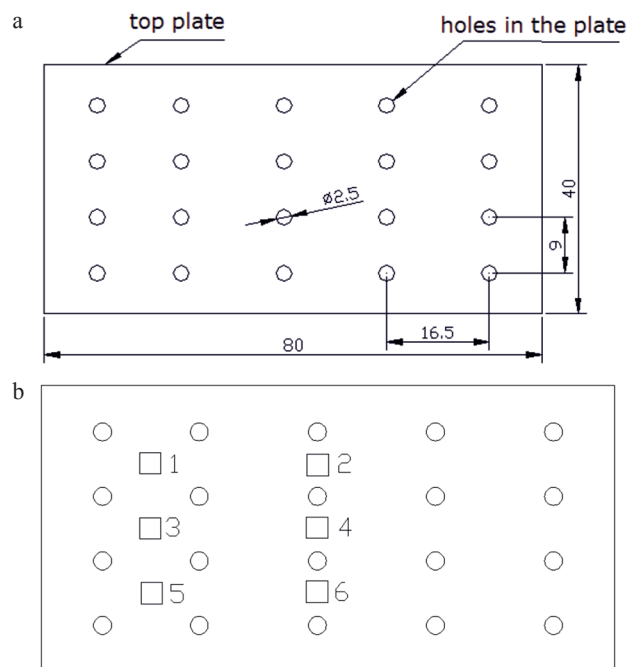


Fig. 1. Distribution of holes for passage of air in RF electrodes: a – distribution of holes on the top plate, b – 6 different positions on the bottom plate (corresponding to their position in top plate) used for heating uniformity tests conducted with carrots (all dimensions are in cm).

Once the samples were heated for the set time and the RF power was turned off, the temperature distribution within the carrot or the radish rectangles was immediately measured using IR imaging. The thermal images of exposed (upper) surface of each layer at the heights of 2, 4, and 6 cm were taken by the infrared thermal imaging camera, beginning from the surface at 6 cm height and working towards the surface at 2 cm height. All of the thermal images were taken within 20 s.

Each treatment was carried out in triplicate and analysis of variance (ANOVA) was performed by applying Duncan tests. SPSS 17.0 software package (SPSS Inc., Chicago, IL, USA) was used to calculate mean values and standard deviations. The standard deviation values were used to construct error bars. The results are reported as mean \pm standard deviation.

RESULTS AND DISCUSSION

The thermal image of temperature distribution within the samples after 5 min of heating in RF (Fig. 2) indicates that the temperature distribution in the entire cross section is almost symmetrical (left to right) which can be attributed to the fact that the electric field in the RF module is symmetrical (left to right). This result indicates that the uniformity of RF heating along the horizontal positions of electrode can be quantified by studying the uniformity on the either side of the symmetry. From this image it can also

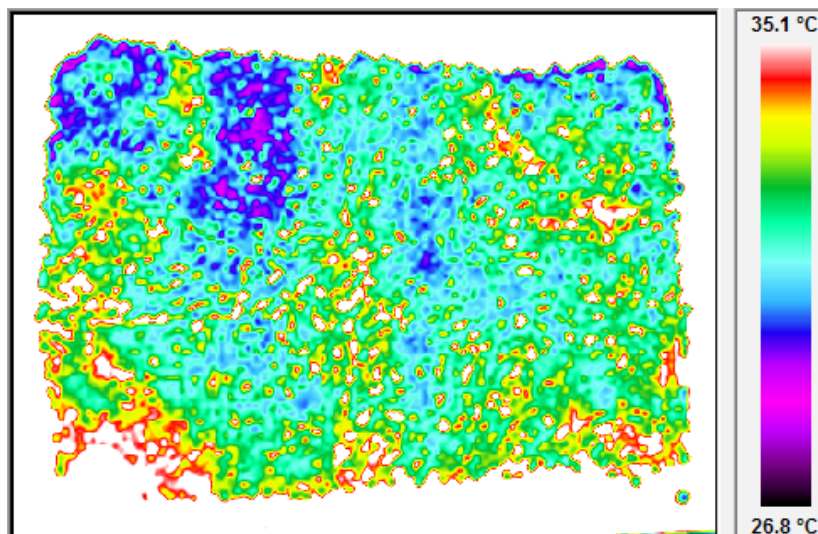


Fig. 2. Thermal image of carrot cubes heated by RF for 5 min.

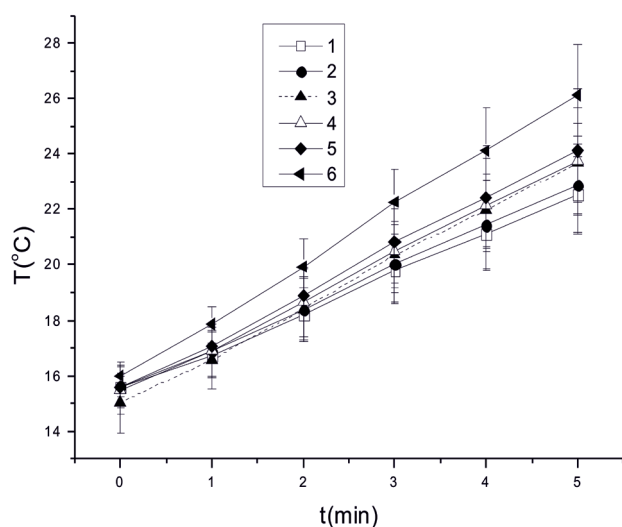


Fig. 3. Temperature history at the different positions (1-6) during the RF heating of carrots cubes for 5 min.

be seen that higher amount of RF energy falls on the edges and corners of the front side of the sample than the back-side. A similar thermal distribution pattern was reported by Huang *et al.* (2015) in the case of soybean where higher intensity of RF energy was observed in corners and edges.

The temperature histories of carrot samples placed at positions 1 to 6 are presented in Fig. 3. As can be observed, the temperature at the position 6 is much more higher compared to that at position 1 and 2 throughout heating. The temperatures values at the remaining positions are between those at position 1 and 6 with temperature at the position 5 is the second highest. This is due to the relatively intense electric field at the front side of the electrode (positions 5 and 6) as compared to that in far end (positions 1 and 2). The highest temperature difference is between position 1 and position 6 which is about 3.6°C at the end of heating. These data points further confirm the temperature distribu-

tion pattern observed in IR images presented in Fig. 3. The temperature variations along positions 1, 3, 5 and positions 2, 4, 6 suggest that moving the samples on a convey belt to the direction of increased intensity of RF could improve the heating uniformity. Liu *et al.* (2013) also reported earlier that moving the conveyor belt along the higher intensity of RF improved the heating uniformity of bread in the RF field. However, the influence of the conveyor speed on heating uniformity was not conclusive in the tested range.

The mean temperature values at three cross-sectional central positions at the height of 1, 3, 5 cm of carrot rectangles ($3 \times 3 \times 6$ cm) during RF heating of 5 min are showed in Fig. 4a. As can be observed, the rate of increase of temperature at the middle layer was the fastest ($0.185^\circ\text{C s}^{-1}$), while it was the slowest ($0.109^\circ\text{C s}^{-1}$) at the top layer and the rate of temperature increase at the bottom layer remained in between ($0.152^\circ\text{C s}^{-1}$). At the end of the 5 min long heating, the temperature at 1cm of height reached as high as about 67.1°C . At the same time the temperatures at 3 and 5 cm heights were 58.7 and 44.2°C , respectively.

The mean temperature values at the heights of 1, 4, and 7 cm, $3 \times 3 \times 8$ cm carrot rectangles for 5 min of RF cavity are studied refer to Fig. 4b. It can also be seen that the temperature and its rate of increase at the vertical middle position are still the highest (93.2°C , and $0.273^\circ\text{C s}^{-1}$). After 5 min of heating, the temperatures at the heights of 1 and 7 cm were 73.2 and 52.3°C , respectively and the rates of temperature increase in these two positions were 0.202 , and $0.136^\circ\text{C s}^{-1}$, respectively.

In Fig. 4c the mean temperature values at the five positions (1, 3, 5, 7, and 9 cm) of $3 \times 3 \times 10$ cm carrot rectangles after 2 min of RF treatment are presented. In these rectangles, comparable temperature and temperature rise rates are achieved within 2 min-long RF heating. The highest temperature (97.2°C) and temperature rise rate ($0.733^\circ\text{C s}^{-1}$) were still achieved at the vertical middle position of the

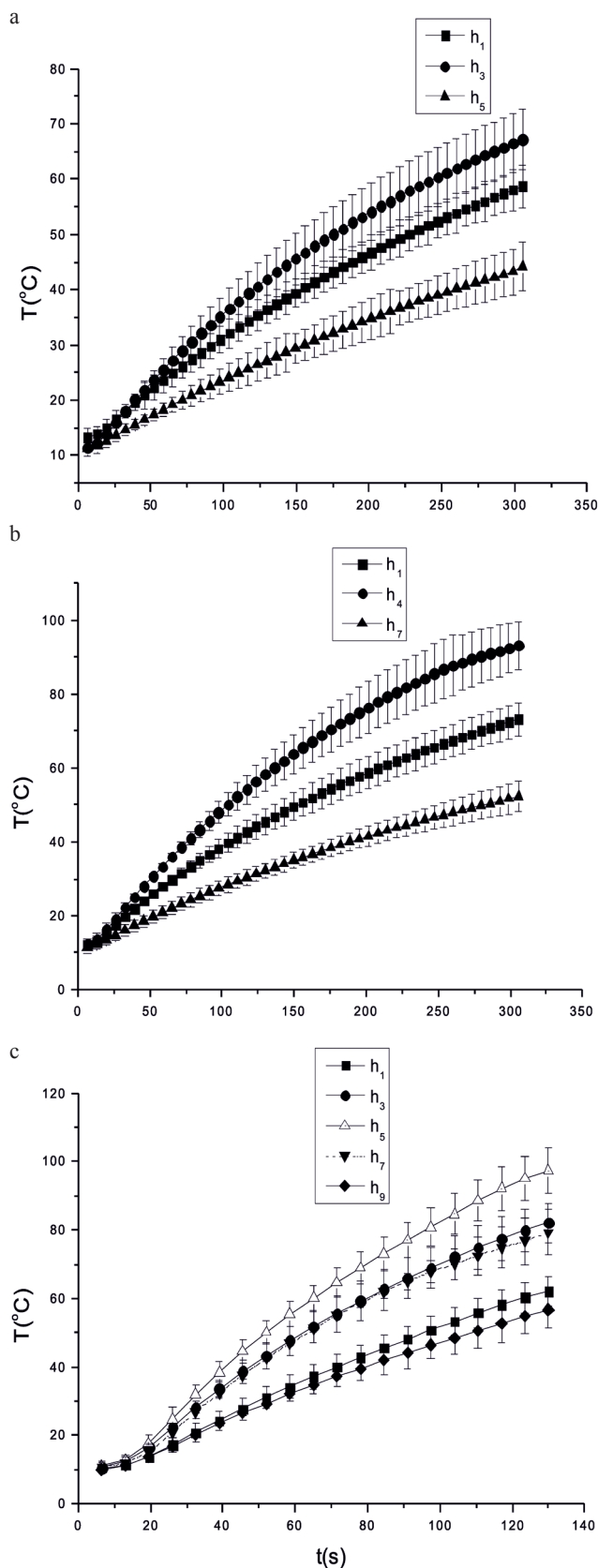


Fig. 4. Temperature at different heights of carrot rectangles: a – at the heights of 1, 3, 5 cm in $3 \times 3 \times 6$ cm, b – at the heights of 1, 4, 7 cm in $3 \times 3 \times 8$ cm, c – at the heights of 1, 3, 5, 7, 9 cm in $3 \times 3 \times 10$ cm.

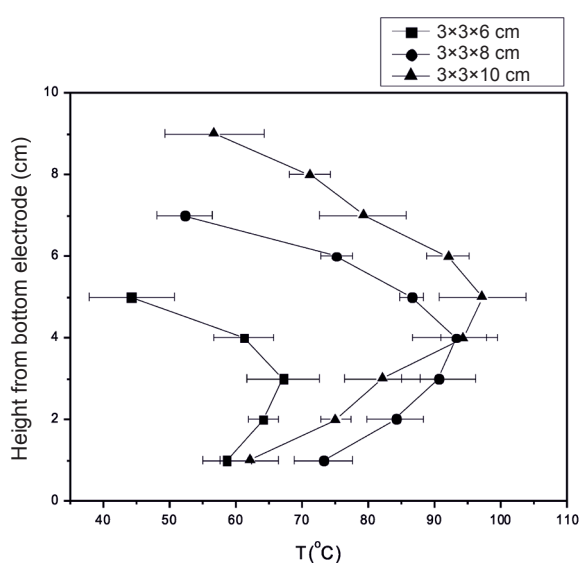
rectangle. The second highest temperature and temperature rise rate were observed at the height of 3 cm (82.1°C and $0.6053^{\circ}\text{C s}^{-1}$). As observed in earlier samples, the temperatures and temperature increase rates at the height of 1 cm were higher than those at the height of 9 cm.

The rates of temperature rise and temperature at the end of heating at the designated heights of different carrot rectangles heated by RF are calculated in Table 1. Accordingly, the temperatures at different vertical positions of carrot rectangles placed at the RF position 4 (Fig. 1) at the end of 5 min ($3 \times 3 \times 6$ cm and $3 \times 3 \times 8$ cm) or 2 min ($3 \times 3 \times 10$ cm) are presented in Fig. 5. The data presented in Table 1 and Fig. 6 further confirm that the temperature and rate of temperature rise are the highest at the vertically central layer in all rectangles. The temperature and the rate of increase of temperature decreased at either higher or lower vertical positions from the vertical central of these rectangles. This non-uniformity of temperature within the sample could be attributed to the unique behaviour of RF electrical field. Similar temperature distribution profiles within samples were reported earlier by Wang *et al.* (2007) in the case of in-shell walnuts. In Wang *et al.* (2007) work, the lowest temperature appeared at the bottom layer when the stacking started at the bottom electrode. When the distance between the top electrode and the top of the stack was equal to the distance between bottom electrode and the bottom stack then the temperature of the top stack was almost similar to that of the bottom stack. These authors opined that the RF generated electrical intensity was higher near the top electrode and it was lower near the bottom electrode. They also opined that the RF generated electrical intensity was almost symmetric about the central plane between the two electrodes. However, higher temperatures were observed at the bottom positions than those at the top positions at the equidistance from the central layer. This difference might have arisen due to the fact that higher heat loss to the ambient air might have occurred from the top since there are unblocked holes on the electrodes of top layer. In this RF module air at ambient temperature was set to blow upwards into the cavity by a fan through the bored holes at the top and bottom electrode to maintain the surface temperature of the samples and protect the samples from overheating. The hole at the bottom electrode was blocked by the Petri dish (used to support the sample) and hence lesser heat loss to the ambient was expected from the bottom layers. Our results are consistent with those of Wang *et al.* (2010, 2014b) as these authors also reported that the temperatures at the bottom positions were slightly higher than those at the top positions when these positions were equidistance about the center. They pointed out that this temperature difference between the bottom and top layers decreased when hot air was combined with RF.

It can be seen from these two figures that the temperature and the rate of increase of temperature at the central position were the highest in the longest rectangle ($3 \times 3 \times 10$ cm)

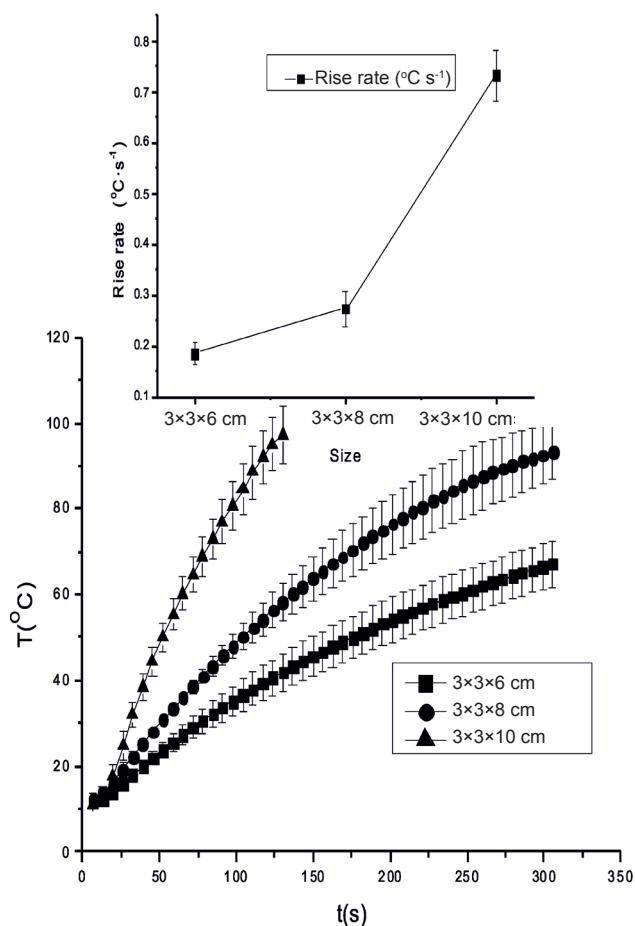
Table 1. Temperature rise rates ($^{\circ}\text{C s}^{-1}$) at different heights of different carrot rectangles

Size (cm)	1	2	3	4	5	6	7	8	9
3×3×6	0.152	0.172	0.185	0.167	0.109	–	–	–	–
3×3×8	0.202	0.248	0.260	0.273	0.249	0.195	0.136	–	–
3×3×10	0.442	0.554	0.605	0.702	0.733	0.694	0.589	0.502	0.392

**Fig. 5.** Temperatures at different heights of carrot rectangles heated with RF for 5 min (3×3×6 cm, 3×3×8 cm) and 2 min (3×3×10 cm).

and they decreased as the length (or height) of the rectangle decreased according to Fig. 6 which shows that the temperature histories and rise rates at the central position of carrot rectangles heated using RF for 5 min (3×3×6 cm, 3×3×8 cm) and 2 min (3×3×10 cm). This fact that the temperature rises faster in taller (higher mass) rectangles than the shorter (lower mass) rectangles of carrots can be used to design RF dryers or sterilizers. Orsat *et al.* processed layers of carrot sticks between parallel plate electrodes (80 mm) in an RF system. They found an increase in the mass of the load brought in better RF coupling. However, this increase in mass resulted into an increase in volume, a change in the shape of the load (from a thin layer to a thicker box shape) and a reduction in the gap between the top surface of the sample and the upper electrode (Orsat *et al.*, 2001).

It can be observed that the trend of distribution of temperature of radish rectangle is similar to that of carrot rectangle except for the fact that the temperatures at similar position and time are much higher in radish rectangle than those in carrot ones refer to Fig. 7. This can be attributed to the lower dielectric constant and loss factor of radish than those of carrot as shown in Materials characterization section. The calculated penetration depths of carrots and radishes are 5.9 and 9.9 cm, respectively. All of this information indicates that the rate of increase of temperature in

**Fig. 6.** Temperature change and rise rates of central point of carrots with different sizes (3×3×6 cm, 3×3×8 cm) and 2 min (3×3×10 cm) during RF treatment for 5 or 2 min.

radish rectangle is expected to be higher than that in carrot rectangle of the same size consistent with the experimental data presented in Fig. 8. The dielectric properties of a material are affected by factors such as frequency, temperature and moisture content (Wang *et al.*, 2005a). Alfaifi *et al.* (2013) determined the dielectric properties of raisins, dates, apricots, figs, and prunes between 10 and 1800 MHz over a temperature range of 20–60°C. They reported that the dielectric constant and loss factor of the above materials decreased with increasing frequency, but increased with increasing temperature at a given frequency. The loss factor of the above mentioned materials increased with the increase in the water content.

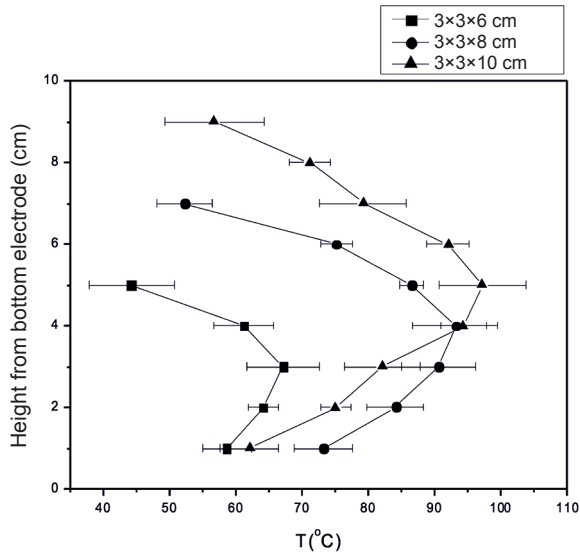


Fig. 7. Temperature at different heights of carrot and radish rectangles of same size ($3 \times 3 \times 8$ cm) measured from bottom electrode at 5 min of RF heating.

The distribution of temperature at the cross sectional area of identical carrot and radish rectangles ($3 \times 3 \times 8$ cm) at different heights starting from the bottom of the RF electrode after heating for 150 s are mapped in Fig. 8. These temperature distribution plots show that at each height the temperatures at the edges and corners are lower than the temperatures at the center which might be due to the loss of heat to the ambient air (Wang *et al.*, 2008, 2014b). These results are contrary to the results reported in the case of RF heating of bread (Liu *et al.*, 2013) and wheat flour (Tiwari *et al.*, 2011a), where the cubic samples had higher RF power densities at the edge than at the center position. In some simulation and prediction of RF heating or thawing of soybean and other food materials, it has been shown that the highest temperature values were observed at the corners and edges at every layer (Huang *et al.*, 2015; Llave *et al.*, 2015; Tiwari *et al.*, 2011b). The higher temperatures at the edges of the RF heated samples are commonly attributed to the field bending and horn effects of the electromagnetic field at interfaces. On the one hand, the different heating

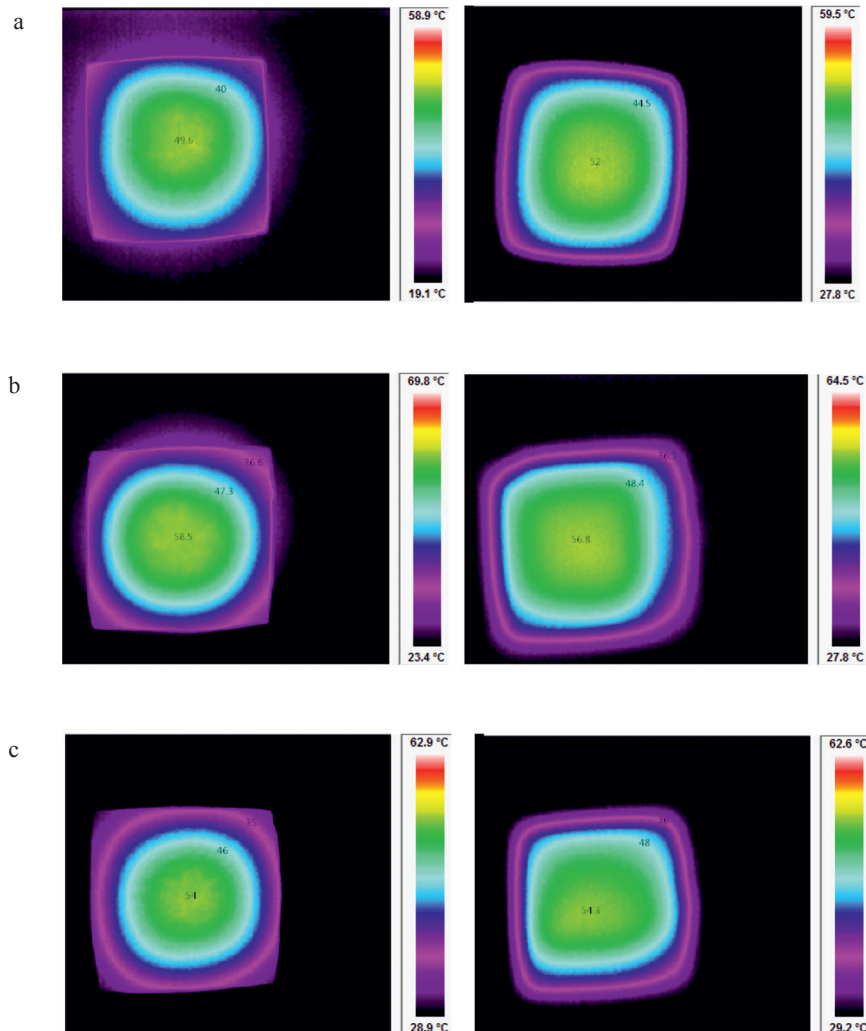


Fig. 8. Temperature images of carrot (left) and radish (right) at different height: a – 6, b – 4, and c – 2 cm from bottom electrode after RF heating of 150 s.

pattern was likely caused by the different materials associated with different dielectric properties and different material volume. The likely cause of the observed lower temperature at the edges than that in the center in both carrot and the radish rectangles, at each height, may be due to the fact that the heat from the edges was promptly transferred to the ambient air and the cooling effect due to heat loss was substantially higher at the edge than at the center.

CONCLUSIONS

1. The temperature distribution in carrot and radish rectangles across the cross sectional area captured by a thermal imaging indicated that the radio frequency field is almost symmetrical within the two electrodes in the radio frequency module used in this study.

2. Heating different sized carrots rectangles and a single sized radish rectangle in an radio frequency cavity indicated that the vertically central positions of the materials were hotter than the points either at higher or lower positions from the vertical center. The temperature of samples at lower positions from the vertical center was higher than the higher positions at equal distance, which was attributed to the greater heat loss to the ambient from the top layers. The rate of rise of temperature was higher in taller (higher mass) carrot rectangles than the shorter (lower mass) ones. The heat penetration in radish rectangle of same size was higher than that in carrot rectangle.

3. The temperatures at the corners and edges of both carrot and radish were found to be lower than their cross sectional center which was attributed to the loss of heat from the corner and edges to the ambient air.

4. The similar trend of temperature distribution across the height and cross section area was observed in carrot and radish samples suggesting that the heating patterns and temperature uniformity in carrots and radishes in RF field are similar.

Conflict of interest: The Authors do not declare conflict of interest.

REFERENCES

- Alfaifi B., Tang J., Jiao Y., Wang S., Rasco B., Jiao S., and Sablani S., 2014.** Radio frequency disinfestation treatments for dried fruit: Model development and validation. *J. Food Eng.*, 120, 268-276.
- Alfaifi B., Wang S., Tang J., Rasco B., Sablani S., and Jiao Y., 2013.** Radio frequency disinfestation treatments for dried fruit: Dielectric properties. *LWT - Food Science and Technology*, 50(2), 746-754.
- Birla S.L., Wang S., and Tang J., 2008a.** Computer simulation of radio frequency heating of model fruit immersed in water. *J. Food Eng.*, 84(2), 270-280.
- Birla S.L., Wang S., Tang J., and Tiwari G., 2008b.** Characterization of radio frequency heating of fresh fruits influenced by dielectric properties. *J. Food Eng.*, 89(4), 390-398.
- Brodie I., 1969.** Calculation of deposition uniformity in rf sputtering. *J. Vacuum Sci. Technol.*, 6(5), 795-800.
- Gao M., Tang J., Johnson J.A., and Wang S., 2012.** Dielectric properties of ground almond shells in the development of radio frequency and microwave pasteurization. *J. Food Eng.*, 112(4), 282-287.
- Gao M., Tang J., Wang Y., Powers J., and Wang S., 2010.** Almond quality as influenced by radio frequency heat treatments for disinfestation. *Postharvest Biology Technol.*, 58: 225-231.
- Ha J.W., Kim S.Y., Ryu S.R., and Kang D.H., 2013.** Inactivation of *Salmonella enterica* serovar *Typhimurium* and *Escherichia coli* O157:H7 in peanut butter cracker sandwiches by radio-frequency heating. *Food Microbiol.*, 34(1), 145-150.
- Huang Z., Zhu H., Yan R., and Wang S., 2015.** Simulation and prediction of radio frequency heating in dry soybeans. *Biosystems Eng.*, 129, 34-47.
- Jiao S., Johnson J.A., Tang J., and Wang S., 2012.** Industrial-scale radio frequency treatments for insect control in lentils. *J. Stored Products Res.*, 48, 143-148.
- Jumah R., 2005.** Modelling and simulation of continuous and intermittent radio frequency-assisted fluidized bed drying of grains. *Food Bioproducts Proc.*, 83(3), 203-210.
- Liu Q., Zhang M., Fang Z.X., and Rong X.H., 2014.** Effects of ZnO nanoparticles and microwave heating on the sterilization and product quality of vacuum packaged Caixin. *J. Sci. Food Agric.*, 94(12), 2547-2554.
- Liu Y., Wang S., Mao Z., Tang J., and Tiwari G., 2013.** Heating patterns of white bread loaf in combined radio frequency and hot air treatment. *J. Food Eng.*, 116(2), 472-477.
- Llave Y., Liu S., Fukuoka M., and Sakai N., 2015.** Computer simulation of radiofrequency defrosting of frozen foods. *J. Food Eng.*, 152, 32-42.
- Luechapattapanorn K., Wang Y., Wang J., Tang J., Hallberg L., and Dunne C., 2005.** Sterilization of scrambled eggs in military polymeric trays by radio frequency energy. *J. Food Sci.*, 70, E288-E294.
- Marra F., Lyng J., Romano V., and McKenna B., 2007.** Radio-frequency heating of foodstuff: Solution and validation of a mathematical model. *J. Food Eng.*, 79(3), 998-1006.
- Marra F., Zhang L., and Lyng J.G., 2009.** Radio frequency treatment of foods: Review of recent advances. *J. Food Eng.*, 91(4), 497-508.
- Orsat V., Bai L., and Raghavan G.S.V., 2004.** Radio-frequency heating of ham to enhance shelf-life in vacuum packaging. *J. Food Process Eng.*, 27, 267-283.
- Orsat V., Garipey Y., Raghavan G.S.V., and Lyew D., 2001.** Radio-frequency treatment for ready-to-eat fresh carrots. *Food Res. Int.*, 34, 527-536.
- Romano V. and Marra F., 2008.** A numerical analysis of radio frequency heating of regular shaped foodstuff. *J. Food Eng.*, 84(3), 449-457.
- Tiwari G., Wang S., Birla S.L., and Tang J., 2008.** Effect of water-assisted radio frequency heat treatment on the quality of 'Fuyu' persimmons. *Biosystems Eng.*, 100(2), 227-234.

- Tiwari G., Wang S., Tang J., and Birla S.L., 2011a.** Analysis of radio frequency (RF) power distribution in dry food materials. *J. Food Eng.*, 104(4), 548-556.
- Tiwari G., Wang S., Tang J., and Birla S.L., 2011b.** Computer simulation model development and validation for radio frequency (RF) heating of dry food materials. *J. Food Eng.*, 105(1), 48-55.
- Ukuku D.O. and Geveke D.J., 2010.** A combined treatment of UV-light and radio frequency electric field for the inactivation of *Escherichia coli* K-12 in apple juice. *Int. J. Food Microbiol.*, 138(1-2), 50-55.
- Uyar R., Bedane T.F., Erdogdu F., Koray Palazoglu T., Farag K.W., and Marra F., 2015.** Radio-frequency thawing of food products – A computational study. *J. Food Eng.*, 146, 163-171.
- Wang L.P., Zhang M., Huang S.B., Lu L.Q., and Roknul Azam S.M., 2014a.** Comparison of three different frequency drying methods for barley chewable tablets. *Drying Technol.*, 32(2), 190-196.
- Wang Y., Zhang L., Gao M., Tang J., and Wang S., 2014b.** Evaluating radio frequency heating uniformity using polyurethane foams. *J. Food Eng.*, 136, 28-33.
- Wang S., Luechapattanaorn K., and Tang J., 2008.** Experimental methods for evaluating heating uniformity in radio frequency systems. *Biosystems Eng.*, 100(1), 58-65.
- Wang S., Monzon M., Gazit Y., Tang J., Mitcham E.J., and Armstrong J.W., 2005a.** Temperature-dependent dielectric properties of selected subtropical and tropical fruits and associated insect pests. *Transactions-american Society Agric. Eng.*, 48, 1873.
- Wang S., Monzon M., Johnson J.A., Mitcham E.J., and Tang J., 2007.** Industrial-scale radio frequency treatments for insect control in walnuts. *Postharvest Biol. Technol.*, 45(2), 240-246.
- Wang S., Tang J., Sun T., Mitcham E.J., Koral T., and Birla S.L., 2006.** Considerations in design of commercial radio frequency treatments for postharvest pest control in in-shell walnuts. *J. Food Eng.*, 77(2), 304-312.
- Wang S., Tiwari G., Jiao S., Johnson J.A., and Tang J., 2010.** Developing postharvest disinfestation treatments for legumes using radio frequency energy. *Biosystems Eng.*, 105(3), 341-349.
- Wang S., Yue J., Tang J., and Chen B., 2005b.** Mathematical modelling of heating uniformity for in-shell walnuts subjected to radio frequency treatments with intermittent stirrings. *Postharvest Biology Technol.*, 35(1), 97-107.